The C-terminal domain of *Drosophila* β_{Heavy}-spectrin exhibits autonomous membrane association and modulates membrane area

Janice A. Williams, Bryce MacIver, Elizabeth A. Klipfell and Claire M. Thomas*

Department of Biology, Department of Biochemistry and Molecular Biology, Eberly College of Science, The Pennsylvania State University, University Park, PA 16802, USA

*Author for correspondence (e-mail: clairet@psu.edu)

Accepted 3 October 2003
Journal of Cell Science 117, 771-782 Published by The Company of Biologists 2004
doi:10.1242/jcs.00922

Summary

Current models of cell polarity invoke asymmetric cues that reorganize the secretory apparatus to induce polarized protein delivery. An important step in this process is the stabilization of the protein composition in each polarized membrane domain. The spectrin-based membrane skeleton is thought to contribute to such stabilization by increasing the half-life of many proteins at the cell surface. Genetic evidence is consistent with a negative role for *Drosophila* β_{Heavy}-spectrin in endocytosis, but the inhibitory mechanism has not been elucidated. Here, we investigated the membrane binding properties of the C-terminal nonrepetitive domain of β_{Heavy}-spectrin through its in vivo expression in transgenic flies. We found that this region is a membrane-association domain that requires a pleckstrin homology domain for full activity, and we showed for the first time that robust membrane binding by such a C-terminal domain requires additional contributions outside the pleckstrin homology. In addition, we showed that expression of the β_{Heavy}-spectrin C-terminal domain has a potent effect on epithelial morphogenesis. This effect is associated with its ability to induce an expansion in plasma membrane surface area. The membrane expansions adopt a very specific bi-membrane structure that sequesters both the C-terminal domain and the endocytic protein dynamin. Our data provide supporting evidence for the inhibition of endocytosis by β_{Heavy}-spectrin, and suggest that the C-terminal domain mediates this effect through interaction with the endocytic machinery. Spectrin may be an active partner in the stabilization of polarized membrane domains.

Key words: Spectrin, Endocytosis, Dynamin, Epithelium, Cell polarity, *Drosophila*

Introduction

The spectrin-based membrane skeleton (SBMS) is a remarkably diverse and multifunctional molecular scaffold that is associated with various cellular membranes. This structure was originally identified as the primary cytoskeletal element in the erythrocyte, where it is responsible for maintaining cell shape and plasma membrane integrity, but it is now recognized as a ubiquitous structure in metazoan cells. The actual and postulated processes in which the SBMS participates include the generation of specialized membrane domains, the polarization of specific proteins in cells, protein sorting, vesicle transport, endocytosis, morphogenesis and even nuclear functions that are yet to be characterized (Bennett and Baines, 2001; De Matteis and Morrow, 2000; Thomas, 2001; Tse et al., 2001). With such diverse functionality, it is not surprising that the SBMS has been shown to play an essential role in development (Dubreuil et al., 2000; Lee et al., 1997; McKeown et al., 1998; Moorthy et al., 2000; Thomas et al., 1998).

The number of integral and peripheral membrane proteins that bind to the SBMS is large and growing (see list in De Matteis and Morrow, 2000). Often, binding is indirect and mediated by adapter proteins with multiple isoforms and specificities, such as ankyrin and protein 4.1, increasing the diversity of possible binding partners (Bennett and Chen, 2001). Interaction with the SBMS can induce polarization of proteins and protein complexes, and it may further serve to stabilize proteins in the membrane by modulating their turnover rate (see, for example, Hammerton et al., 1991). The presence of the SBMS juxtaposed to the membrane may additionally influence the protein composition of a membrane in more subtle ways by corralling unattached proteins into 'compartments' created by the network through stearic hindrance of lateral diffusion (Sako and Kusumi, 1995), and/or by posing a barrier to endocytosis (Kamal et al., 1998). Because multiple spectrin isoforms tend to define mutually exclusive membrane regions (Bennett and Baines, 2001), these observations indicate that the SBMS is likely to have a significant role in maintaining protein polarity.

Spectrins are heterotetrameric proteins comprising two α and two β chains. Each chain is a long, rope-like molecule, consisting largely of triple α-helical repeat units of 106 amino acids each (Speicher and Marchesi, 1984; Thomas et al., 1997), with specialized protein modules within, and at either end of this array. α- and β-spectrins dimerize in an antiparallel fashion and dimer pairs bind via a 'head-to-head' interaction to generate tetramers (Tse et al., 1990). This arrangement leaves an actin-binding domain at either end of the tetramer, enabling spectrin to crosslink actin into branched networks associated

with membrane surfaces (Bennett and Baines, 2001). β-spectrins are categorized into 'conventional' β and 'heavy' β_H isoforms that differ primarily in their number of spectrin repeats (17 and 30, respectively). In invertebrates, both β isoforms dimerize with a common α-chain and show a clear segregation along the apicobasal axis in epithelia: β_H is confined to the apical domain in most cells, whereas conventional β-spectrin is found only in the basolateral domain (Dubreuil et al., 1997; Thomas and Williams, 1999), making this an ideal model to answer questions about the role of the SBMS in cell polarity. A comprehensive description of this role requires an understanding of the activities of the SBMS, as well as the mechanism(s) by which the different spectrin isoforms stably associate with their respective domains.

β-spectrin subunits appear to contain the most potent and specific membrane association domains within the tetramer. First, the best-characterized β-spectrin-membrane association lies in segments 16/17 of conventional β-spectrin where the adapter molecule ankyrin mediates the interaction with many integral membrane proteins (Bennett and Chen, 2001; Kennedy et al., 1991). Such associations seem to be an important organizational pathway for the association with, or organization of, some specific membrane domains (see, for example, Jenkins and Bennett, 2001). Second, the N-terminal actin binding domain of β-spectrin binds to integral membrane proteins via other adapter proteins such as protein 4.1 and α-catenin (Marfatia et al., 1997; Pradhan et al., 2001). Third, nonerythroid β-spectrins contain a C-terminal phospholipid-binding pleckstrin homology (PH) domain, conferring on them a direct site of association with the membrane (De Matteis and Morrow, 2000).

The rules by which such membrane interactions lead to the polarized assembly of a spectrin network remain unclear. At the plasma membrane, cell contact provides an extrinsic cue that recruits some SBMS to polarized locations. In Madin-Darby canine kidney cells, the SBMS is closely associated with cadherin-based adhesion (Nelson et al., 1990), possibly mediated by α-catenin (Pradhan et al., 2001). Intrinsic cues must also exist for spectrin to become localized to the Golgi (De Matteis and Morrow, 2000) and to regions such as the terminal web (Hirokawa et al., 1983; Thomas et al., 1998). In the fly, the apical β_H spectrin is closely associated with *D*E-cadherin-mediated contacts (Thomas and Williams, 1999; Thomas et al., 1998), whereas the L1 class cell adhesion molecule (L1-CAM) neuroglian recruits the basolateral SBMS via an ankyrin link to β-spectrin (Dubreuil et al., 1997).

β_{Heavy}-spectrin isoforms do not bind to ankyrin (Coleman et al., 1989; Lee et al., 1997; Thomas et al., 1997), indicating that other interactions must mediate its recruitment to the membrane. We have previously reported that mutations in the *karst* locus, which produce truncated β_H isoforms lacking the C-terminus and tetramerization site, do not detectably accumulate at the plasma membrane in epithelial cells (Medina et al., 2002; Zarnescu, 2000) (Fig. 1A). This suggests that the C-terminal half of the molecule contains sequences that are necessary for membrane association. Three essential activities might be missing from these truncated proteins (see Fig. 1): (1) a requirement for network formation via the tetramerization domain (segment 32), (2) β_H-protein interactions mediated by the missing repeats and/or the C-terminal nonrepetitive segment 33, and (3) β_H-phospholipid interactions mediated by the pleckstrin homology (PH) domain within segment 33. Given the dominant role of the C-terminal PH domain region for ankyrin-independent interaction with the membrane in conventional β-spectrin isoforms (Davis and Bennett, 1994; Lombardo et al., 1993), we have investigated membrane interactions mediated by the homologous β_H segment 33. We show that β_H segment 33 exhibits autonomous localization to the plasma membrane in vivo, but that this region cannot recapitulate the wild-type β_H distribution. Although the PH domain itself is an important part of this membrane binding activity, other protein-protein interactions are additionally required for stable association with the plasma membrane. We also show that overexpression of the C-terminus results in a dominant defect resulting in an increase in plasma membrane area. This defect appears to be in an endocytic pathway since the membrane expansion phenotype is associated with sequestration of dynamin. Our data suggest, for the first time, that the SBMS may be an active participant in regulating membrane turnover by nucleating a complex on segment 33 of β_H that modulates endocytosis, thus stabilizing the associated membrane domain.

Materials and Methods

Construction of transgenes expressing derivatives of β_H segment 33.

To create pβH33, a fragment containing codons 3560-4097 of the β_H coding region was excised from the cDNA pBH12 (Thomas and Kiehart, 1994) using *Nae*1 and *Eco*R1 and cloned into pUAST (Brand and Perrimon, 1993), along with an N-terminal myc-tag (Munro and Pelham, 1987). The transgene is under the control of the Gal4 binary expression system and silent unless crossed to a Gal4-expressing driver line (Brand and Perrimon, 1993). To create deletion derivatives a PCR approach was used and all fragments were cloned into pUAST with an N-terminal myc-tag as above. For βHPH+5-3 primers PH-A (5′-ACAAGCGGCGTGAGATTTACGAAC-3′) and PH+3EX (5′-AGAATTCTCTAGAAAGGAATGCCATTTGGGGAGT-3′) were used to generate a fragment encompassing β_H codons 3560 to 3920. For pβHPH+3 the primers BHPH5 (5′-CACCCGTTGAGATT-CAG-3′) and PH+3EX (see above) were used to generate a fragment from pBH12 encompassing codons 3747 to 3920. To eliminate the PH domain in pβH33ΔPH, two pairs of primers were used to generate fragments flanking the PH domain. PHA (see above) and PHB (5′-TGTTCGGCAGGTCGAATCCTTCACCCTTCT-3′) produced the 5′ flanking fragment; PHC (5′-GGAATTCGGTGGCGCTCC-TTCTCATTGT-3′) and PHD (5′-TCGACCTGCCGAACATGC-AACTGCTTAGC-3′) produced the 3′ flanking fragment. These two fragments were mixed, and used as a PCR template with the two distal primers PHA and PHC, resulting in a fragment containing codons 3560-3746 followed by 3858-4097. A PCR strategy was also followed to create the β-spectrin segment 19 derivative βspPH using the primers BspPH (5′-ATGTTGGTGCCTCGCACGAC-3′) and Bsp3 (5′-AGAATTCTCTAGATTACTTTTTCTTTAAAGTAAAAAAC-3′). The resulting protein contains amino acids 2131-2291 of β-spectrin. All PCR fragment clones were sequence-verified before cloning into pUAST.

Fly stocks

Flies were maintained on standard cornmeal-agar food with all crosses carried out at defined temperatures to standardize Gal4 expression levels. Following sequence verification, transgenic fly lines containing pβH33, pβHPH+3, pβHPH+5-3, pβH33ΔPH and pβspPH were created by standard methods (Rubin and Spradling, 1982), and are

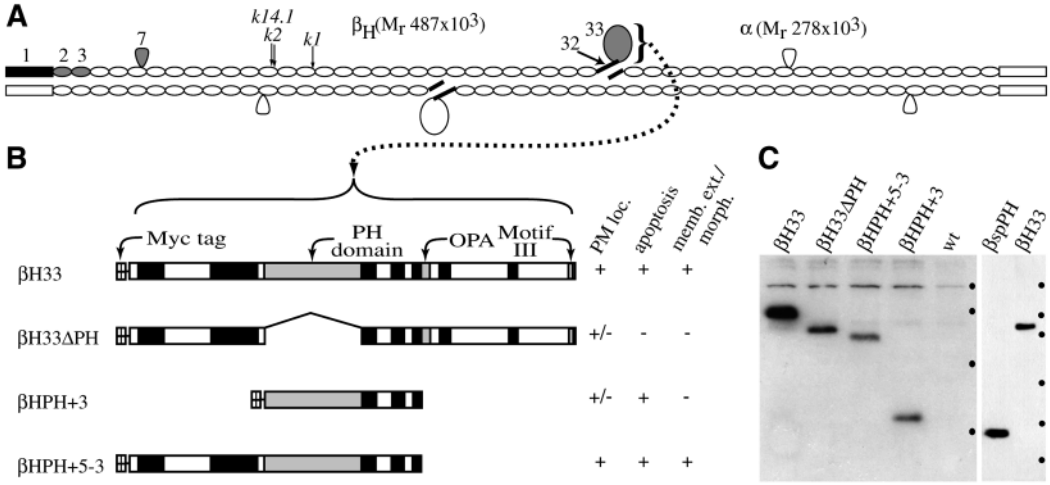

Fig. 1. Transgenic constructs derived from the β_{Heavy}-spectrin C-terminal segment 33. (A) An $(\alpha\beta_H)_2$ tetramer. Known functional domains are indicated by their segment number: 1, actin binding domain; 2,3, αβ dimer nucleation site; 7, Src homology 3 domain; 32, tetramerization site; 33, nonrepetitive C-terminal domain containing the pleckstrin homology (PH) domain. For further details on these domains see Thomas et al. (Thomas et al., 1997) and references therein. Also illustrated are the approximate locations of the truncations arising from the three *karst* alleles kst^1, kst^2 and $kst^{14.1}$ (Medina et al., 2002). (B) Subdomains within segment 33 (βH33) and its derivatives described in this paper. Myc-tag, epitope for the 9E10 antibody (Munro and Pelham, 1987). Gray boxes, PH domain (pleckstrin homology domain); OPA, short polyglutamine repeat (Wharton et al., 1985); motif III, lysine-rich repeat found at the C-terminus of most β-spectrins (Lombardo et al., 1993). Black boxes indicate regions conserved (=10 amino acid stretches exhibiting ⩾50% identity) in comparison with the *Anopheles* homologue of β_H. βH33ΔPH, βHPH+3 and βHPH+5-3 are described in the text. PM loc. indicates the ability of each construct to exhibit stable plasma membrane localization; apoptosis indicates the ability of each construct to induce apoptosis in some tissues; memb. ext./morph. indicates the ability of each construct to inhibit salivary gland invagination and induce the bi-membrane structures described in this paper. (C) Expression of the proteins illustrated in B. Two immunoblots are shown of extracts derived from the heads of adults expressing spectrin derivatives under the control of the GMR-Gal4 driver in the eye. Ten heads were used for each lane, and both blots were probed with the mAb 9E10 to detect the N-terminal myc-tag. Lanes are labeled for the construct expressed (see B) or wt (wild-type). The left-hand blot shows that each construct is expressed and migrates at their predicted size. Marker migration is indicated by black dots for 97, 68, 43 and 29 kDa (top to bottom). The right-hand blot shows the expression of βspPH (see text), with βH33 for reference. Marker migration is indicated by black dots for 220, 98, 66, 46, 30 and 14 kDa (top to bottom).

designated *P{w^{+mc} kst$^{βH33.Scer\UAS.T:Hsap\MYC}$=pβH33}*, *P{w^{+mc} kst$^{βHPH+3.Scer\UAS.T:Hsap\MYC}$=pβHPH+3}*, *P{w^{+mc} kst$^{βHPH+5-3.Scer\UAS.T:Hsap\MYC}$=pβHPH+5-3}*, *P{w^{+mc} kst$^{βH33ΔPH.Scer\UAS.T:Hsap\MYC}$=pβH33ΔPH}* and *P{w^{+mc} β-spec$^{βspPH.Scer\UAS.T:Hsap\MYC}$=pβspPH}*, respectively. The driver lines *P{w$^{+mW.hs}$=GawB}185Y* and *P{w$^{+mW.hs}$=GawB}69B*, as well as the *P{w^{+mC}=UAS-p35}* line and the LacZ reporter line *P{w^{+mC}=UAS-lacZ.NZ}J312* were obtained from the Bloomington Stock Center (Bloomington, IN). The driver line *P{w^{+mC}=fkh-Gal4}* was obtained from D. Andrew (Johns Hopkins University, MD). The *P{w^{+m*}=Gal4-vg}* (F. M. Hoffman, University of Wisconsin, Madison, WI) and *P{w$^{+mW.hs}$=GawB}C96* (Gustafson and Boulianne, 1996) were obtained from E. Siegfried (Penn State, PA). The *P{GMR-p35}* line (Hay et al., 1994) was obtained from G. Rubin (University of California at Berkeley, CA). The *P{w^{+mC}=GMR-Gal4}* driver line (Freeman, 1996) was obtained from Z. Lai (Penn State, PA).

Antibodies

Antibodies were used at the following concentrations: mouse monoclonal anti-c-myc (Ab-1; clone 9E10; Oncogene Research Products, San Diego, CA) was used at [1:100]. Rabbit anti-α-spectrin (#354), mouse-monoclonal anti-α-spectrin (ascites #N3) and rabbit anti-β-spectrin (#89; all from D. Branton, Harvard University, Cambridge, MA) were used at [1:500], [1:1000] and [1:200], respectively (Byers et al., 1987). Affinity purified rabbit anti-β_H was prepared as previously described (Thomas et al., 1994), and used at [1:100]. Mouse monoclonal anti-*D*Moesin and rabbit anti-*D*Moesin (D. Kiehart, Duke University, Durham, NC) were used at [1:500] and [1:10,000], respectively. Rabbit anti-clathrin (mosquito; A. Raikhel, Michigan State University, East Lansing, MI) was used at [1:100]. Rabbit anti-Stranded at second (D. Cavener, Penn State, University Park, PA) was used at [1:500]. Rabbit anti-dynamin (#2074 and #Shi3; M. Ramaswami, University of Arizona, Phoenix, AZ) were used at [1:200]. Rabbit anti-Amphiphysin (A Zelhof, University of California San Diego, La Jolla, CA) was used at [1:100]. Rat anti-*D*Creb-A (D. Andrew, Johns Hopkins University, Baltimore, MD) was used at [1:15,000]. Mouse monoclonal anti-β-galactosidase (Promega; Madison, WI) was used at [1:2000]. Alexa546-anti-mouse and Alexa488-anti-rabbit secondary antibodies (Molecular Probes; Eugene, Oregon USA) were used at [1:250].

Microscopy

Embryo fixation and staining for immunofluorescence followed standard methods. Embryos were imaged using an Olympus Fluoview 300 microscope (Olympus America, Melville, NY). Embryos were prepared for electron micrcoscopy according to Tepass and Hartenstein (Tepass and Hartenstein, 1994) and imaged on JEOL transmission electron microscope (JEM 1200 EXII, Peabody, MA).

Acridine orange staining of imaginal discs

Wing imaginal discs from late 3rd instar larvae raised at 22°C were dissected in PBS and immediately transferred to a 2 μM solution of Acridine Orange in PBS for 3-5 minutes at room temperature. Following a wash in PBS to remove excess stain, discs were mounted in PBS and imaged by epifluorescence.

Bi-membrane image analysis

Image analysis of the bi-membranes closely resembled that of Lambert et al. (Lambert et al., 1997) and were performed on a Macintosh computer using the public domain program Image J v1.29x

(developed at the U.S. National Institutes of Health and available on the Internet at http://rsb.info.nih.gov/nih-image/). Digital images of bi-membranes were examined for stretches where both component bilayers were visible for some distance. Five such regions totaling 1.27 μm of bi-membrane (range 147-318nm) were selected manually, straightened using the macro 'Straighten Curved Objects' (Kocsis et al., 1991), and contrast stretched. Image J was then used to generate a density profile across each example, and the numerical values were transferred to Microsoft Excel vX (Microsoft Corporation, Mountain View, CA) to be averaged and plotted. The final plot (see Fig. 6G) represents a sample of >3000 transects.

Results

Given the enormous size of β_H (M_r~480×10^3), we chose a transgenic approach to investigate the presence of membrane binding and polarization activities in segment 33 (Fig. 1A). The last 528 amino acids of β_H were cloned along with an N-terminal myc-tag (Munro and Pelham, 1987), downstream of the heterologous UAS promoter (Fig. 1B; see Materials and Methods). This protein, referred to as βH33, and a series of deletion derivatives, were assayed for membrane localization and dominant effects in vivo (Fig. 1B). On expression of *P{pβH33}* and its derivatives, proteins of the expected size could be detected in tissue homogenates using an anti-myc antibody (Fig. 1C).

Overexpression of the β_{Heavy}-spectrin segment 33 induces apoptosis in some tissues

Transfection of transgenes expressing fragments of β-spectrin in vertebrate Caco-2 cells has been previously reported to cause the progressive loss of expressing cells from the culture (Hu et al., 1995), so we began by expressing βH33 in a variety of tissues to see if cell lethality also occurs in *Drosophila*. Crossing this construct to various Gal4-expressing driver lines showed that expression of βH33 often has a catastrophic effect on development. Expression at modest levels in the ectoderm (69B-Gal4 driver) resulted in substantial pupal lethality, with pharate adults exhibiting limb truncations and reduced wing size suggestive of a cell lethal effect or a defect in proliferation (data not shown). Tissue-specific expression at the wing margin (C96-Gal4 or *vg*-Gal4 drivers) produced notching (Fig. 2A,B), whereas expression in the late 3rd instar eye disc during eye differentiation (GMR-Gal4 driver) caused disorganization of the eye (Fig. 2D,E). These effects were independent of the particular βH33 insertion used and could be modulated by temperature (a Gal4 effect), with an increasing and more extensive loss of morphology seen at higher temperatures. Together, these data indicate that these phenotypes result from expression of the βH33 protein itself and not from the disruption of a gene at the insertion site.

Two experiments indicate that the underlying cause of the wing and eye phenotypes is an increase in the rate of apoptosis. First, acridine orange staining of freshly dissected 3rd instar wing imaginal discs expressing βH33 under the control of the *vg*-Gal4 driver caused a prominent accumulation of dye along cells of the wing margin, coincident with the domain of highest Gal4 expression, and was not seen in control discs (Fig. 2G,H). Second, co-expression of βH33 in the differentiating eye (GMR-Gal4 driver) or wing (*vg*-Gal4 driver), along with the baculovirus caspase inhibitor, p35 (Hay et al., 1994), produced a conspicuous reduction in severity of both the wing and eye defects (Fig. 2C,F).

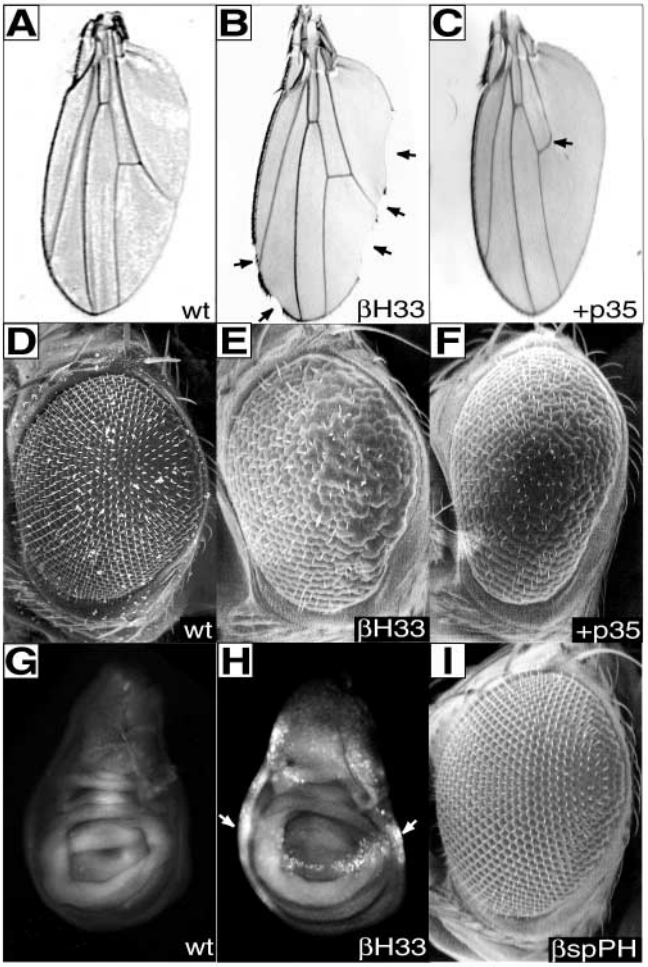

Fig. 2. Expression of β_H segment 33 induces apoptosis in imaginal tissues. (A) Wild-type wing. (B) Notches (arrows) resulting from the expression of βH33 under the control of the *vg*-Gal4 driver along the wing margin. (C) βH33-induced notching is rescued by co-expression of the baculovirus p35 caspase inhibitor from a UAS-p35 transgene. Curiously, vein L5 (arrow) is incomplete in such wings. (D) Scanning electron micrograph (SEM) of a wild-type eye. (E) SEM of an eye resulting from the expression of βH33 under the control of the GMR-Gal4 driver in the developing eye disc at 20°C, which produces an intermediate phenotype. (F) The rough eye phenotype shown in E is rescued by co-expression of the baculovirus p35 caspase inhibitor from a GMR-p35 transgene. (G) Live wild-type 3rd instar wing disc stained with acridine orange to reveal cells undergoing apoptosis. (H) Live 3rd instar wing disc expressing βH33 under the control of the *vg*-Gal4 driver stained with acridine orange. Numerous dying cells are detected in the region of greatest βH33 expression along the wing margin (arrows). (I) SEM of a typical eye resulting from the expression of the β-spectrin C-terminal derivative βspPH under the control of the GMR-Gal4 driver at 25°C. Only a mild phenotype composed of a few mispositioned bristles is seen despite abundant protein expression (Fig. 1C).

This apoptotic phenotype is produced by the proteins βH33, βHPH+3 and βHPH+5-3, but not βH33ΔPH, implicating the PH domain and sequences to its immediate C-terminal side in the induction of apoptosis (Fig. 1B; data not shown). To test

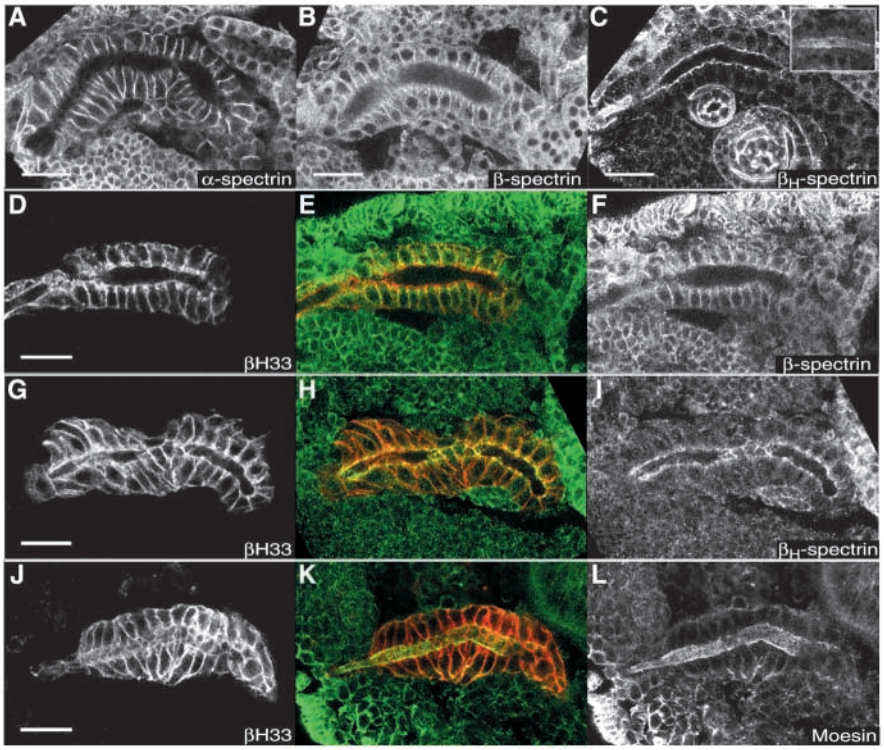

Fig. 3. β_H segment 33 exhibits autonomous membrane localization. Sagittal confocal sections of salivary glands are shown in A-I. A parasagittal section in the plane of the lumenal surface is shown in J-L. All embryos are between stages 13 and 16. (A) A wild-type salivary gland stained for α-spectrin. (B) A wild-type salivary gland stained for β-spectrin. (C) A wild-type salivary gland stained for β_H-spectrin. Inset, parasagittal image at the lumenal surface. (D-L) Salivary glands expressing βH33 under the control of the *fkh*-Gal4 driver. Glands are costained for βH33 with mAb 9E10 and anti-β-spectrin (D-F), anti-β_H (G-I) or anti-*D*Moesin (J-L) antibodies. In each case staining for βH33 is shown on the left (red in the merged image) with the second protein on the right (green in the merged image). Bars, 20 μm.

the specificity of the apoptotic effect of β_H segment 33, we overexpressed part of the homologous C-terminal segment 19 from conventional fly β-spectrin (βspPH; Fig. 1C) that is equivalent to the minimal region of βH33 that causes apoptosis (i.e. βHPH+3). βspPH thus contains a similar PH domain to βHPH+3, but is divergent in its neighboring sequences. βspPH expression was essentially benign, producing only a very mild eye phenotype consisting of a few mispositioned bristles (Fig. 2I). Because the β-spectrin and β_H C-termini share a similar PH domain, this result indicates that βH33-induced apoptosis is unlikely to arise from sequestration of phospholipid alone. This result also shows that the apoptotic phenotype is specific to β_H, and further suggests that the PH domain *plus* neighboring sequences to its C-terminal side are responsible for this effect.

The β_{Heavy}-spectrin C-terminus exhibits autonomous localization to the membrane

The embryonic salivary gland appears to be insensitive to the apoptotic effects of the β_H C-terminal constructs, permitting a unique opportunity to characterize the membrane localization properties of these proteins. The gland is a well-polarized tubular epithelium that is favorable for studying morphogenesis and the location of polarized membrane proteins (Bradley et al., 2001). We began by characterizing the localization of α-, β- and β_H-spectrin in wild-type glands. α-spectrin was present along the entire lateral membrane encompassing both the apical junctional region and the basolateral domain (Fig. 3A), whereas β-spectrin and β_H were confined to the basolateral and apical domains, respectively (Fig. 3B,C). Interestingly, β_H was found at both the apicolateral margin of the cells and across the free apical surface (Fig. 3C inset), whereas α-spectrin was not present at detectable levels at the free apical surface, suggesting that β_H is being recruited independently to this domain.

The salivary gland-specific Gal4-drivers, 185Y and *fkh* (see Materials and Methods), were used to express βH33 and its derivatives in this tissue. *fkh*-Gal4 drives the expression of transgenes in the salivary gland anlagen before invagination of the cells, and continues expression throughout embryonic development. By contrast, 185Y-driven expression begins after invagination and is limited to the secretory region of the gland.

Immunofluorescent staining for βH33 using the anti-myc monoclonal antibody (mAb) 9E10 revealed that this protein appears initially in the cytoplasm, but becomes localized to the cell membrane within a few minutes, where it persists throughout embryogenesis (Fig. 3). The βH33 distribution is found at varying levels throughout the plasma membrane. It is most prominent along the lateral membrane, where it colocalizes with β- and β_H-spectrins (Fig. 3D-I), and is slightly enriched in the apicolateral β_H/junctional region (Fig. 3G-I). βH33 is also present at low levels across the apical domain where it colocalizes with the apical marker *D*Moesin (Fig. 3J-L). Thus, βH33 exhibits an autonomous membrane localization activity that overlaps with, but is not restricted to, the normal β_H domain at the apicolateral margin. The polarity of endogenous β_H must therefore require the presence of other sequences outside this C-terminal region.

Multiple contributions are required for the stable membrane localization of the β_H segment 33

To examine the sequence contributions to membrane binding within β_H segment 33, we compared the localization of a series of deletion derivatives (Fig. 1B). First, we examined the contribution of the β_H PH domain to its membrane-targeting ability by expressing the deletion construct, βH33ΔPH (Fig. 1B,C). While clearly retaining some ability to associate with the membrane, this construct exhibited higher cytoplasmic levels and less robust membrane localization than βH33,

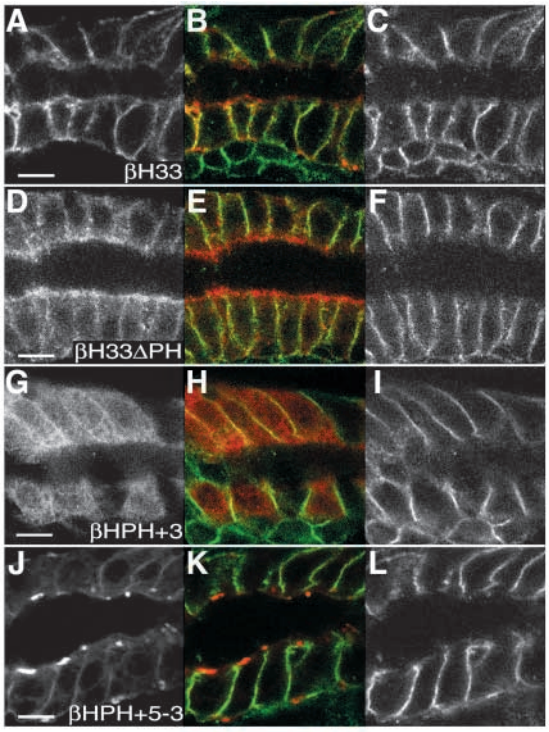

Fig. 4. Deletion analysis reveals multiple contributions to the membrane binding of β_H segment 33. Sagittal confocal sections of salivary glands expressing βH33 and its derivatives (Fig. 1B) under the control of the 185Y-Gal4 driver. All images show costaining for the β_H derivative using the mAb 9E10 (left panel, red in merged image) and α-spectrin (right panel, green in merged image). Embryos are at stage 14-16. (A-C) Costaining for βH33. (D-F) Costaining for βH33ΔPH. (G-I) Costaining for βHPH+3. (J-L) Costaining for βHPH+5-3. Bars, 10 μm.

indicating that it has a reduced membrane association activity (compare Fig. 4A,D). Although this result suggests that phospholipid binding is important for membrane association by β_H segment 33, the probable presence of an overlapping protein binding site (Fig. 1B), as reported for other PH domains (see, for example, Touhara et al., 1995), complicates this interpretation. Interestingly, βH33ΔPH appears to be somewhat concentrated in the apical cytoplasm, although the reason for this is currently unknown.

To determine whether the PH domain is sufficient for membrane association, we attempted to express this domain in isolation, but could not detect this protein either by immunoblot or immunofluorescence when expressed in flies (data not shown). However, the inclusion of protein sequences to the C-terminal side of the PH domain up to, but not including, the OPA sequence (βHPH+3; Fig. 1B) resulted in a protein that is readily detected (Fig. 1C). Immunolocalization of this derivative in the salivary gland reveals a strong cytoplasmic distribution, with weak membrane binding (Fig. 4G-I), similar to that of βH33ΔPH (Fig. 4D-F). These results indicate that the PH domain is important, but not sufficient, for stable membrane association.

Because βHPH+3 does not stably associate with the plasma membrane, additional regions of segment 33 must be required for the stable membrane association exhibited by βH33. The inclusion of protein sequences to the N-terminal side of the PH domain (βHPH+5-3; Fig. 1B) resulted in a protein that is capable of stable membrane association (Fig. 4J-L). Initially, βHPH+5-3 had low cytoplasmic levels and appeared on the lateral membrane with a slight enrichment in the apicolateral margin (data not shown). However, it subsequently accumulated in large protrusions that initially emerged from the apicolateral region in each cell (Fig. 4J). These structures were also found less frequently in the basal domain, where they also tend to emerge from the periphery, and they are occasionally seen at the lateral membrane. Similar protrusions are seen with prolonged expression of βH33; however, βHPH+5-3 caused the formation of these protrusions with much greater potency.

Together, these results indicate that the PH domain is important for the membrane association of βH33 but that other regions contribute to the membrane binding exhibited by this domain. Furthermore, given that the complete segment 33 (βH33) is not overtly polarized along the apicobasal axis, our results suggest that the apical polarity of β_H must be conferred by additional interactions (e.g. with Crumbs).

The membrane protrusions associated with β_H segment 33 comprise a distinct membrane domain containing the endocytic GTPase dynamin

The βH33 and βHPH+5-3 membrane protrusions can become quite large (e.g. Fig. 5A,J). Costaining for βHPH+5-3 and the apical marker Stranded at second reveals a mutually exclusive distribution for these two proteins on the lumenal surface (Fig. 5A-F). The apical surface of the salivary gland contains β_H, and its associated proteins Crumbs (Myat and Andrew, 2002) and *D*Moesin (Fig. 3L); however, neither β_H (data not shown) nor *D*Moesin (Fig. 5G-I) accumulates in these structures, indicating that these concentrations of βH33 and βHPH+5-3 are not part of the normal cortical cytoskeleton, but rather represent a distinct domain.

Examination of these protrusions by transmission electron microscopy reveals that they are huge membranous extensions that fold across the cell surface (Fig. 6A,B,E), or appear as rolled circular structures (Fig. 6C,D). This observation suggests that the βH33 and βHPH+5-3 derivatives, which exhibit stable membrane association, are interfering with the normal regulation of the cells' surface area.

The fine structure of these membrane extensions, which we term bi-membranes, is informative. Each bi-membrane is a closely adherent pair of lipid bilayers. In sections where the point of emergence from the cell surface is visible, the lipid bilayer on either side is seen to merge into a bi-membrane, by juxtaposition and adhesion of their inner (cytoplasmic) leaflets. Such bi-membranes remain closely opposed with a fairly uniform spacing of 8.7 nm (Fig. 6F,G). In the case of 'flat' extensions lying on the cell surface, the distal ends of the bi-membranes often open into loops, and exhibit occasional separations of the component bilayers (arrowhead in Fig. 6E). Both appear to contain cytoplasmic material that presumably became trapped during extrusion.

There are three classes of circular membrane protrusion. The first sits on the apical surface, may contain the distinctive fibrous material from the lumen of the gland, and simply represents a coiled version of the flat bi-membranes (not

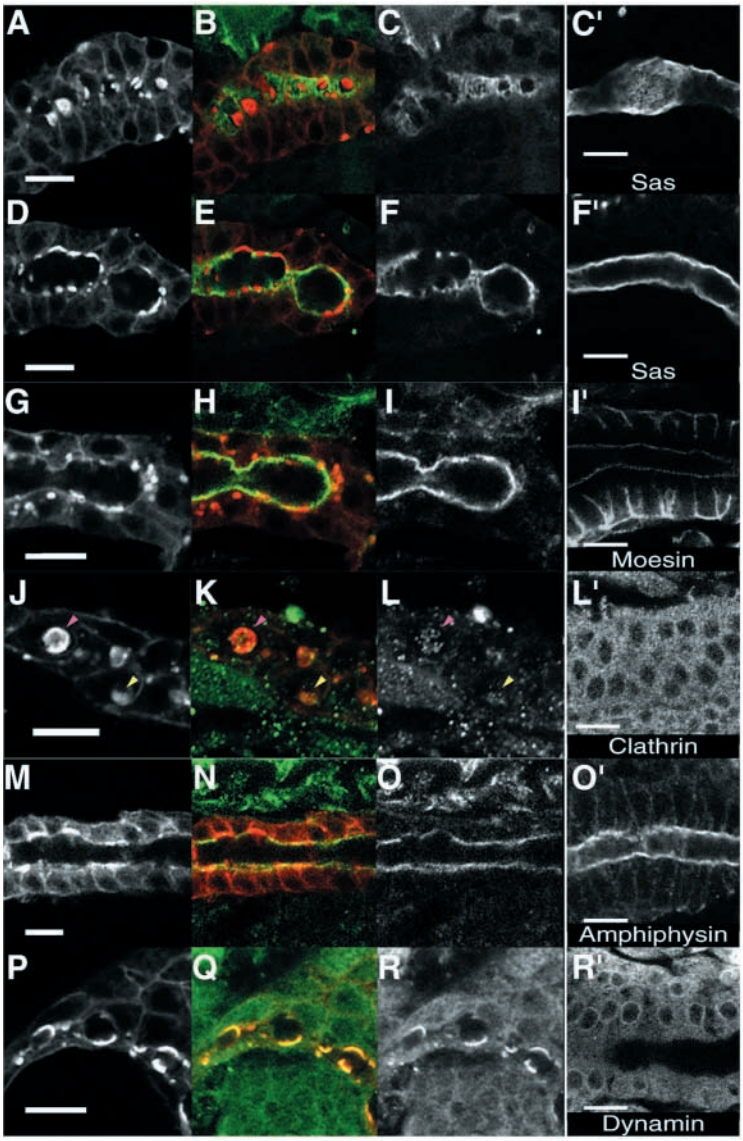

Fig. 5. Overexpression of β_H segment 33 generates a distinct membrane domain associated with dynamin. (A-R) Costaining for β_H derivative βHPH+5-3 using mAb 9E10 (left panel, red in merged image) and various membrane markers (right panel, green in merged image). All embryos are at stage 15. (A-F) Costaining for the apical transmembrane protein Stranded at second (Sas). (A-C) A parasagittal section at the level of the lumenal surface. (D-F) Sagittal section of the same gland. (G-I) Costaining for the apical cortical protein *D*Moesin. (J-L) Costaining for the endocytic protein clathrin. Clathrin puncta (see arrowheads) are seen in arrangements that suggest some association with the membrane protrusions. (M-O) Costaining for the endocytic protein amphiphysin. (P-R) Costaining for the protein dynamin (Shibire). (C′,F′,I′,L′,O′,R′) Comparable stainings of wild-type glands for the same antigen as in C, F, I, L, O and R, respectively. Bars, 20 μm.

shown). The other two classes appear in the cytoplasm, and are both surrounded by a single membrane bilayer on their cytoplasmic side (see interpretive drawings in Fig. 6C,D). Such circular forms often adhere to the inner surface of the plasma membrane (Fig. 6C). Of these, one class contains cytoplasmic material in its central space surrounded by a normal bilayer (Fig. 6C), which we presume to be the same as the terminal loops seen at the ends of the flat bi-membranes. The third type contains lumenal material surrounded by a bi-membrane, indicating that such structures are contiguous with the lumen (Fig. 6D). The path of the bi-membranes in these complex structures always becomes indistinct at one or more positions around their circumference. These positions may represent transitions between layers that are tilted relative to the plane of sectioning. Because bi-membranes are seen to plunge back into the cytoplasm pulling in the plasma membrane on either side, it seems likely that the circular forms in the cytoplasm are actually coiled intrusions from the plasma membrane.

Genetic studies have implicated a Crumbs/β_H complex in the regulation of apical membrane area, possibly by regulating endocytosis (Pellikka et al., 2002). We therefore stained salivary glands expressing βH33 and βHPH+5-3 for several markers to see if these bi-membrane structures were endocytic in origin. Clathrin and amphiphysin do not accumulate to high levels in these structures (Fig. 5J-O), although there does seem to be a loose association with clathrin puncta in some confocal planes (Fig. 5J-L). However, the large GTPase dynamin (Shibire), which catalyzes the final separation of endocytic vesicles from the membrane, accumulates to high levels and shows co-extensive staining with the β_H C-terminal constructs that produce these structures (Fig. 5P-R). This observation suggests that βH33 and βHPH+5-3 dominantly interfere with membrane recovery from the cell surface, leading to membrane accumulation as secretion continues.

β_H segment 33 overexpression dominantly disrupts salivary gland morphogenesis

Recent data have indicated that the regulation of membrane turnover is generally important for morphogenesis (Lecuit and Pilot, 2003), and is specifically required for salivary gland development (Myat and Andrew, 2002). Therefore, it is not surprising that the β_H C-terminal constructs βH33 and βHPH+5-3, which cause the accumulation of the bi-membrane structures, have a significant impact on the development of the salivary gland. If expression of βHPH+5-3 is driven by the 185Y-Gal4 line, and thus is expressed after the salivary gland anlagen becomes fully internalized, the glands typically appear elongated, with aberrant cell morphologies and irregular lumenal diameters. At embryonic stage 16 no lengthening is evident, with both wild-type and mutant glands stretching for about 22% of the embryo length (wt 22.1±2.2% (n=11); mutant 22.0±4.2% (n=8); P=0.95). However, by late stage 16 or stage 17 the mutant glands are on average 11% longer (wt 23.1±1.0% (n=13); mutant 25.6±0.9% (n=32); P=0.002). A comparison of the mean number of nuclei in normal and mutant glands revealed a slight difference (wild-type 112.5±6.2 (n=8); mutant 124.0±4.5 (n=17); P=0.012). However, the more dispersed mutant nuclei were easier to count at deeper focal planes and so the wild-type estimates may represent a slight undercount.

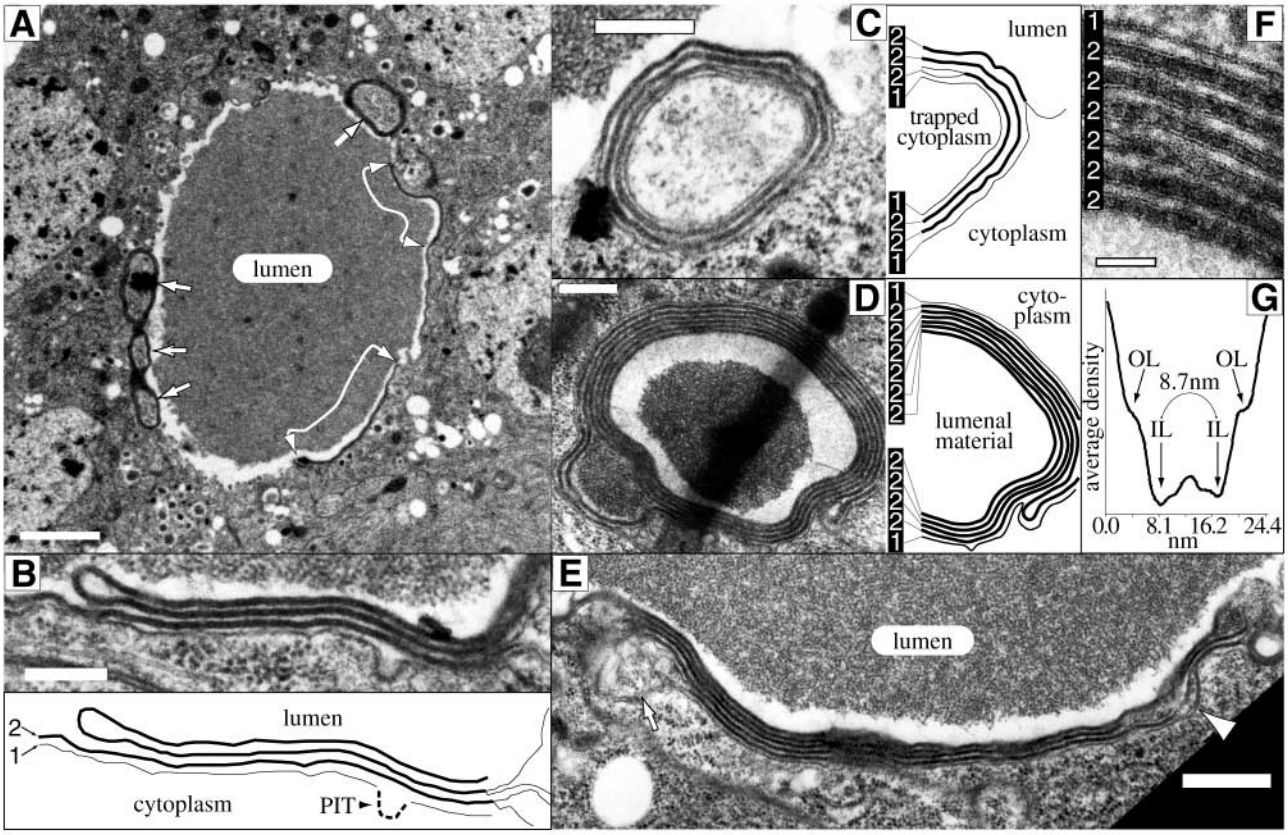

Fig. 6. The β_H segment 33-induced membrane domains have a distinctive bi-membrane topology. All images are transmission electron micrographs of stage 14-16 embryonic salivary glands expressing βHPH+5-3 under the control of the *fkh*-Gal4 driver. (A) Low-magnification cross-sectional view of the apical end of salivary gland cells and lumen. Arrows indicate circular bi-membrane structures. Linked arrows delimit the ends of large bi-membrane sheets lying on the apical surface. Bar, 2 μm. (B) Higher-magnification view of a flat bi-membrane structure where one bi-membrane folds back on itself. In the interpretive drawing below, thin lines represent single membrane bilayers; thick lines represent bi-membranes. A single membrane bilayer is always seen at the cytoplasmic side of these stacks and is presumed to be the apical surface. PIT, mid-stage clathrin coated pit. Bar, 250 nm. (C) Circular bi-membrane within the cytoplasm, but closely opposed to the apical plasma membrane. This structure appears to have cytoplasm trapped in its center. An interpretive drawing is to the right. Note how the pattern of single bilayers (thin lines numbered 1) and bi-membranes (thick lines numbered 2) is 2,2,2,1 on the lumenal side and 1,2,2,1 on the cytoplasmic side, indicating that the outermost membrane is adhering to form a bi-membrane with the inner leaflet of the apical membrane. Bar, 300 nm. (D) Circular bi-membrane within the cytoplasm that is not against the plasma membrane in this section. This structure has lumenal material in its center. An interpretive drawing is to the right. In contrast to the structures filled with cytoplasm, the enclosed lumenal material is delimited by a bi-membrane (lines numbered as in C). This, along with the lumenal content, indicates that the center of this structure is contiguous with the lumenal surface of the gland. Bar, 300 nm. (E) A more complex stack of bi-membrane folds lying on the apical surface. Separation of the component bilayers is often seen at the end of the surface bi-membranes (arrow) and occasionally along their length (arrowhead). Typically, such separations contain material resembling cytoplasm. Bar, 500 nm. (F) High-magnification view of part of the circular structure shown in D. Here, the bilayer (1)/ bi-membrane (2) structure is clearly visible. Apart from occasional sites of cytoplasmic inclusion, the individual bilayers in each bi-membrane closely parallel one another. Bar, 50 nm. (G) The plot shows an average density profile across imaged bi-membranes with the positions of the cytoplasmic inner leaflet (IL) and extracellular outer leaflet (OL) indicated (see Materials and Methods). The inner leaflets have an average separation of 8.7 nm.

To clarify this issue, we stained embryos expressing βHPH+5-3 for mitotic figures using anti-phosphohistone H3. As wild-type salivary gland cells do not proliferate after invagination begins (Bradley et al., 2001), the observation of any mitotic figures would be an indication of excess proliferation. Despite robust staining of proliferating cells in other tissues, careful examination of 50 embryos, ranging in stage from 13 to 17, revealed no mitotic figures in any region of the salivary glands (data not shown). Together, these data strongly indicate that overproliferation does not contribute to this elongated morphology.

Using the *fkh*-Gal4 driver line, cell invagination begins normally at the dorsal posterior region of the anlagen (data not shown) (Bradley et al., 2001), but later arrests, leaving many cells on the surface of the embryo (Fig. 7). The internalized cells migrate to their normal position (Fig. 7C, bracket 1), whereas those left on the surface are carried forwards during head involution and remain as a mass at the anterior (Fig. 7C, bracket 2). The degree to which cell invagination is successful appears to be related to the rate at which these segment 33 derivatives accumulate, as comparison of one- and two-insert transgenic lines reveals a more severe phenotype in the latter. The cells that remain on the surface retain their apicobasal polarity, and staining for the apical lumenal marker *D*Moesin

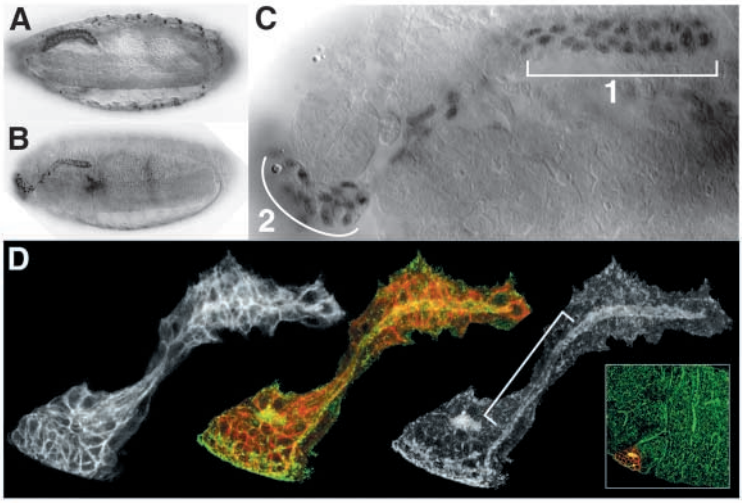

Fig. 7. β_H segment 33 dominantly interferes with salivary gland development. (A) A stage 16 wild-type embryo expressing a nuclear UAS-LacZ marker and stained for β-galactosidase protein to illustrate the normal position and morphology of the gland. (B) A stage 16 embryo co-expressing a nuclear UAS-LacZ marker and βHPH+5-3 under the control of the *fkh*-Gal4 driver and stained for β-galactosidase protein. Expression before invagination prevents complete internalization, with cells that remain on the surface being swept forwards to the head region during head involution. (C) Higher-magnification photomontage of the gland shown in B. Note how the posterior cells that first internalized resolutely assume their normal position (bracket 1), and that relatively few cells extend to the location of the cells that do not internalize (bracket 2). (D) Projected confocal series of a salivary gland from a stage 13 embryo expressing βHPH+5-3 under the control of the *fkh*-Gal4 driver. The embryo was stained for βHPH+5-3 (left image, red in merged center panel) using the mAb 9E10 and for the lumenal marker *D*Moesin (right image, green in merged center panel). For clarity in the projection, the 9E10-staining region was used as a guide to select *D*Moesin staining that is in the gland cells. *D*Moesin staining is actually very widespread (inset shows the uncropped outermost section from the series; see also Fig. 3L). Bracket indicates the continuity of the lumen revealed by *D*Moesin staining.

reveals that a continuous lumen exists from the surface through to the internalized portion of the gland (Fig. 7D, bracket). As the cells remaining on the surface continue to express the salivary gland-specific fkh-Gal4 driver (Fig. 7B,C) and *D*Creb-A transcription factor (Bradley et al., 2001) (data not shown), it is unlikely that any cell fate change has occurred in these cells. Moreover, cuticle preparations on such embryos that are allowed to develop to a late stage exhibit an absence of cuticle at their anterior end where the cell mass resides (data not shown). Together, these results indicate that the cells fail to internalize because they are incapable of normal morphogenesis, and not because they have become epidermal.

Discussion

Contemporary models of cell polarity invoke the cortical cytoskeleton as a stabilizing influence on asymmetric membrane domains (see, for example, Yeaman et al., 1999). Here, we investigated the membrane binding properties of the β_{Heavy}-spectrin (β_H) C-terminal segment 33. We showed that this domain autonomously localizes to the plasma membrane and, as expected from the analysis of vertebrate homologs, we found that the pleckstrin homology (PH) domain is an important contributor to membrane binding. However, we also found that membrane binding conferred by the β_H PH domain is augmented by other interactions. In addition, we showed that expression of β_H segment 33 has a dominant effect on cell morphology and epithelial development. This dominant phenotype is associated with dramatic overgrowths of the plasma membrane that sequester the endocytic protein dynamin. These data support the proposed role of β_H as a downregulator of endocytosis (Pellikka et al., 2002; Zarnescu, 2000) and therefore a stabilizing factor for its associated membrane domains.

β_{Heavy}-spectrin C-terminal segment 33 is a membrane association domain

Previous data suggest that the C-terminal nonrepetitive domain of nonerythroid β-spectrins is an important site of ankyrin-independent membrane association (Davis and Bennett, 1994; Lombardo et al., 1993) that functions by association with the phospholipid phosphatidylinositol-4,5-bisphosphate via a PH domain (Hyvonen et al., 1995; Rameh et al., 1997; Zhang et al., 1995). Different isoforms of β-spectrin have markedly divergent sequences surrounding this motif, which may also contribute to membrane attachment. β_H-spectrins do not associate with ankyrin, but they do contain a canonical spectrin PH domain, and such ankyrin-independent association may be an important contributor to membrane binding by the heavy isoforms.

The in vivo localization data presented here suggests that phospholipid binding is a necessary function of the β_H C-terminal membrane association domain because deletion of the PH domain disrupts membrane association. However, the PH domain plus its immediate C-terminal sequences did not exhibit robust membrane localization, indicating that neither phospholipid binding nor overlapping protein binding (Touhara et al., 1995) is sufficient for stable plasma membrane association. This suggests that phospholipid binding is part of a more complex anchoring mechanism, possibly serving a regulatory role.

β_H segment 33 does not exhibit conspicuous polarity, showing that it is unlikely to direct full-length β_H to its apical domain. Recently, we and others have shown that β_H is recruited to the membrane by the apical polarity determinant Crumbs, and that null *crumbs* alleles dominantly enhance the phenotype arising from C-terminal truncations of β_H (Medina et al., 2002; Pellikka et al., 2002) (Fig. 1A). These results suggested that Crumbs binds to the N-terminal half of β_H, or to α-spectrin. However, the avidity with which these truncated proteins bind to the membrane is low, as little if any is detectable at the membrane (Zarnescu, 2000; Zarnescu and Thomas, 1999). This indicates that Crumbs-association is not sufficient for β_H-membrane binding and that more C-terminal parts of the protein must contribute through other interactions. The data presented here are consistent with a model in which Crumbs provides a polarized anchor for β_H, whereas the C-terminus contributes to its stable membrane association. However, the role of other sequences missing in the *karst* mutants must additionally be examined.

In this context, it is interesting to find that β_H is apparently recruited to the apical membrane of the salivary gland in the absence of α-spectrin. Other reports are beginning to indicate a significant degree of independence between the membrane binding of α- and β- or β_H-spectrins (Lopez-Schier and St Johnston, 2002; Norman and Moerman, 2002; Dubreuil et al., 2000; Dubreuil and Yu, 1994). Together, such data raise the possibility that the requirement for an α/β network per se among nonerythroid SBMS (Deng et al., 1995) may be a domain-specific feature, or secondary to membrane association.

Multiple functions of β_H segment 33

Expression of β_H segment 33 causes a dominant apoptotic phenotype in susceptible tissues, whereas it disrupts epithelial morphogenesis and causes a membrane expansion phenotype elsewhere. These appear to represent two distinct functions, given that they are dependent on different sequences within the domain. The apoptotic phenotype requires the PH domain plus sequences to its C-terminal side and is specific to β_H, as it is not seen on expression of the equivalent β-spectrin fragment, and presumably reflects some aspect of the protein-lipid interactions defined by the βHPH+3 construct. By contrast, the inhibition of morphogenesis and the induction of membrane expansion require additional protein interactions mediated by the sequences on the N-terminal side of the PH domain. This multiplicity of effects complicates the interpretation of genetic interaction experiments; however, current data are most consistent with βH33 causing a gain-of-function phenotype. Thus, *karst* alleles do not dominantly enhance the βH33 phenotype, whereas β_H overexpression is additive or synergistic, and β_H is not displaced by βH33 expression (J.A.W., I.B.M. and C.M.T., unpublished). Clearly, there is much complexity within this region of the β_H molecule.

β_{Heavy}-spectrin segment 33 modulates membrane area

The C-terminal segment 33 of β_H causes a phenotype that is consistent with the potent inhibition of endocytosis, resulting in the sequestration of dynamin at the membrane. Given that we have observed these extensions in both the salivary gland (this paper) and trachea (J.A.W., E.A.K. and C.M.T., unpublished), this is not a salivary gland specific effect, and thus reflects a more general function of β_H.

The SBMS has been suggested to facilitate membrane stability and cell polarity by limiting the lateral diffusion of proteins to sites of endocytosis and as a physical barrier to clathrin pit formation (Hammerton et al., 1991; Sako and Kusumi, 1995; Kamal et al., 1998). In addition, a few reports of binding between SBMS proteins and endocytic components have also hinted at a more active role for the SBMS during endocytosis (Cianci et al., 1995; Macoska et al., 2001; Michaely et al., 1999). Our results support the idea that the SBMS stabilizes membrane domains by regulating membrane turnover, and extends these models by suggesting that the apical SBMS actively regulates protein turnover by nucleating a protein complex that modulates endocytosis. A primary role of this activity may be to downregulate endocytosis in order to stabilize the protein composition of the associated membrane – a role that would fit well with models of cell polarity (Yeaman et al., 1999). Thus, the polarizing cues that recruit β_H (Fig. 8A, pathway 1) may do so in part, to modulate endocytosis via segment 33 (Fig. 8A, pathway 2).

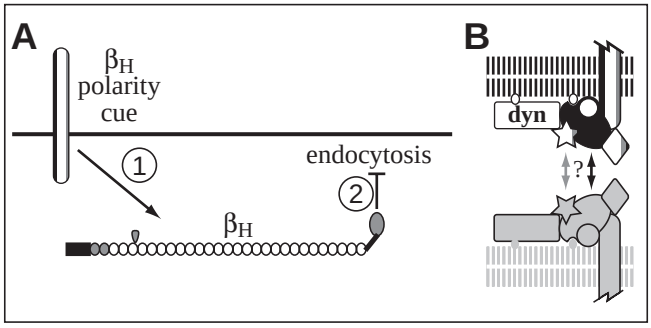

Fig. 8. Models for the action of β_H segment 33. (A) We suggest that polarized membrane cues recruit β_H (pathway 1) in part to use β_H segment 33 to inhibit endocytosis and thus stabilize that domain (pathway 2; see text for discussion). (B) A model for the origin of the bi-membrane structures caused by β_H expression. We suggest that β_H segment 33 (black oval) is in a complex with one or more proteins (including dynamin (dyn)) and that self association between β_H segment 33 (gray arrows) or an associated protein (black arrows) leads to adhesion between the inner leaflets of the plasma membrane.

β_H collaborates with Crumbs, and an unidentified partner of Crumbs, to modulate the area of the photoreceptor apical stalk domains in the eye (Pellikka et al., 2002). It is not known if Crumbs acts to stimulate membrane delivery or to inhibit recovery, or both. On the basis of the data presented here, we would suggest that Crumbs recruits β_H to downregulate endocytosis. β_H could play a similar stabilizing role at adherens junctions, supporting the notion that the disruption of the ZA seen in *karst* mutants (Zarnescu and Thomas, 1999) could arise from the inappropriate turnover of junctional components (Zarnescu, 2000).

Crumbs activity and the modulation of apical surface area have been shown recently to be important factors in the morphogenesis of the salivary gland (Myat and Andrew, 2002). Given that the turnover of junction proteins is required for epithelial morphogenesis (Tepass et al., 1996; Uemura et al., 1996), we speculate that β_H segment 33 expression inhibits cell internalization because of its inhibitory role in endocytosis. Importantly, the membrane extensions cannot be a physical barrier to morphogenesis, as cell internalization ceases before their emergence. Whether there is a causal relationship between β_H segment 33 inhibition of endocytosis and cell internalization will be the subject of future investigations.

Crumbs also recruits the cortical actin organizer Moesin (Medina et al., 2002), and *moesin* mutations cause apical membrane overgrowth (Speck et al., 2003). However, loss-of-function *moesin* alleles (Polesello et al., 2002) do not eliminate β_H from the membrane in follicle cells (J.A.W. and C.M.T., unpublished), and so parallel modulation of membrane area by *D*Moesin and β_H seems probable.

β_H segment 33-induced membrane extensions have a distinctive bi-membrane topology

The presence of dynamin, but not clathrin or amphiphysin in the β_H-induced membrane extensions, suggests that the endocytic process being inhibited is either clathrin-

independent or is occurring in the later stages of clathrin-mediated endocytosis. The appearance of apparently normal mid-stage coated pits in our samples (e.g. arrow in Fig. 6B) is consistent with both of these notions. Whichever pathway is inhibited, there must be a structural transition that releases dynamin from its tubular 'pinching' assemblies into these more lamellar structures.

We regard the bi-membranes to be a chronic symptom of the inhibition of endocytosis by β_H segment 33, but their structure is nonetheless informative. The morphology of the membranes clearly indicates that β_H segment 33 is either capable of self-association leading to membrane adhesion, or that it is associated with a protein with this property (Fig. 8B). The dimensions of the bi-membrane are strongly reminiscent of membrane junctions produced by annexins (Gerke and Moss, 2002; Lambert et al., 1997). Furthermore, annexinVI has been associated with the proteolytic removal of spectrin to facilitate clathrin-mediated endocytosis in vertebrate cells (Kamal et al., 1998). Therefore, we speculate that a fly homologue of one of these annexin proteins is normally associated with the apical SBMS, and mediates the formation of these bi-membrane structures through a regulatory or structural association with β_H segment 33. We are currently generating antibody and genetic reagents to test this hypothesis.

We would like to thank our numerous colleagues (see Materials and Methods) and the Bloomington Stock Center for supplying antibodies and fly stocks; Robert Coleman, John Fisher, Aaron Gitler, Hilary Oman, Missy Hazen, Elaine Kunze, Susan Magargee, Michelle Peiffer and Rosemary Walsh for technical assistance; Esther Siegfried, Deborah Andrew and members of the Thomas lab for critically reading this manuscript; and Douglas Cavener and Channa Reddy for their support. J.A.W. was supported by NIH fellowship GM20906. This work was funded in part by NIH grant GM52506.

References

Bennett, V. and Baines, A. J. (2001). Spectrin and ankyrin-based pathways: metazoan inventions for integrating cells into tissues. *Physiol. Rev.* **81**, 1353-1392.

Bennett, V. and Chen, L. (2001). Ankyrins and cellular targeting of diverse membrane proteins to physiological sites. *Curr. Opin. Cell Biol.* **13**, 61-67.

Bradley, P. L., Haberman, A. S. and Andrew, D. J. (2001). Organ formation in Drosophila: specification and morphogenesis of the salivary gland. *BioEssays* **23**, 901-911.

Brand, A. H. and Perrimon, N. (1993). Targeted gene expression as a means of altering cell fates and generating dominant phenotypes. *Development* **118**, 401-415.

Byers, T. J., Dubreuil, R., Branton, D., Kiehart, D. P. and Goldstein, L. S. (1987). Drosophila spectrin. II. Conserved features of the alpha-subunit are revealed by analysis of cDNA clones and fusion proteins. *J. Cell Biol.* **105**, 2103-2110.

Cianci, C. D., Gallagher, P. G., Forget, B. G. and Morrow, J. S. (1995). Unique subsets of proteins bind the SH3 domain of α1 spectrin and GRB2 in differentiating mouse erythroleukemia (MEL) cells. *Mol. Biol. Cell* **6s**, 217a.

Coleman, T. R., Fishkind, D. J., Mooseker, M. S. and Morrow, J. S. (1989). Contributions of the beta-subunit to spectrin structure and function. *Cell Motil. Cytoskeleton* **12**, 248-263.

Davis, L. H. and Bennett, V. (1994). Identification of two regions of beta G spectrin that bind to distinct sites in brain membranes. *J. Biol. Chem.* **269**, 4409-4416.

De Matteis, M. A. and Morrow, J. S. (2000). Spectrin tethers and mesh in the biosynthetic pathway. *J. Cell Sci.* **113**, 2331-2343.

Deng, H., Lee, J. K., Goldstein, L. S. and Branton, D. (1995). Drosophila development requires spectrin network formation. *J. Cell Biol.* **128**, 71-79.

Dubreuil, R. R. and Yu, J. (1994). Ankyrin and beta-spectrin accumulate independently of alpha-spectrin in Drosophila. *Proc. Natl. Acad. Sci. USA* **91**, 10285-10289.

Dubreuil, R. R., Maddux, P. B., Grushko, T. A. and MacVicar, G. R. (1997). Segregation of two spectrin isoforms: polarized membrane-binding sites direct polarized membrane skeleton assembly. *Mol. Biol. Cell* **8**, 1933-1942.

Dubreuil, R. R., Wang, P., Dahl, S., Lee, J. and Goldstein, L. S. (2000). Drosophila beta spectrin functions independently of alpha spectrin to polarize the Na,K ATPase in epithelial cells. *J. Cell Biol.* **149**, 647-656.

Ferguson, K. M., Kavran, J. M., Sankaran, V. G., Fournier, E., Isakoff, S. J., Skolnik, E. Y. and Lemmon, M. A. (2000). Structural basis for discrimination of 3-phosphoinositides by pleckstrin homology domains. *Mol. Cell* **6**, 373-384.

Freeman, M. (1996). Reiterative use of the EGF receptor triggers differentiation of all cell types in the Drosophila eye. *Cell* **87**, 651-660.

Gerke, V. and Moss, S. E. (2002). Annexins: from structure to function. *Physiol. Rev.* **82**, 331-371.

Gustafson, K. and Boulianne, G. L. (1996). Distinct expression patterns detected within individual tissues by the GAL4 enhancer trap technique. *Genome* **39**, 174-182.

Hammerton, R. W., Krzeminski, K. A., Mays, R. W., Ryan, T. A., Wollner, D. A. and Nelson, J. W. (1991). Mechanism for regulating cell surface distribution of Na^+, K^+-ATPase in polarized epithelial cells. *Science* **254**, 847-850.

Hay, B. A., Wolff, T. and Rubin, G. M. (1994). Expression of baculovirus P35 prevents cell death in *Drosophila*. *Development* **120**, 2121-2129.

Hirokawa, N., Cheney, R. E. and Willard, M. (1983). Location of a protein of the fodrin-spectrin-TW260/240 family in the mouse intestinal brush border. *Cell* **32**, 953-965.

Holt, R. A., Subramanian, G. M., Halpern, A., Sutton, G. G., Charlab, R., Nusskern, D. R., Wincker, P., Clark, A. G., Ribeiro, J. M., Wides, R. et al. (2002). The genome sequence of the malaria mosquito Anopheles gambiae. *Science* **298**, 129-149.

Hu, R.-J., Moorthy, S. and Bennett, V. (1995). Expression of functional domains of beta$_G$-spectrin disrupts epithelial morphology in cultured cells. *J. Cell Biol.* **128**, 1069-1080.

Hyvonen, M., Macias, M. J., Nilges, M., Oschkinat, H., Saraste, M. and Wilmanns, M. (1995). Structure of the binding site for inositol phosphates in a PH domain. *EMBO J.* **14**, 4676-4685.

Jenkins, S. M. and Bennett, V. (2001). Ankyrin-G coordinates assembly of the spectrin-based membrane skeleton, voltage-gated sodium channels, and L1 CAMs at Purkinje neuron initial segments. *J. Cell Biol.* **155**, 739-746.

Kamal, A., Ying, Y. and Anderson, R. G. (1998). Annexin VI-mediated loss of spectrin during coated pit budding is coupled to delivery of LDL to lysosomes. *J. Cell Biol.* **142**, 937-947.

Kennedy, S., Warren, S., Forget, B. and Morrow, J. (1991). Ankyrin binds to the 15th repetitive unit of erythroid and non-erythroid beta-spectrin. *J. Cell Biol.* **115**, 267-277.

Kocsis, E., Trus, B. L., Steer, C. J., Bisher, M. E. and Steven, A. C. (1991). Image averaging of flexible fibrous macromolecules: the clathrin triskelion has an elastic proximal segment. *J. Struct. Biol.* **107**, 6-14.

Lambert, O., Gerke, V., Bader, M. F., Porte, F. and Brisson, A. (1997). Structural analysis of junctions formed between lipid membranes and several annexins by cryo-electron microscopy. *J. Mol. Biol.* **272**, 42-55.

Lecuit, T. and Pilot, F. (2003). Developmental control of cell morphogenesis: a focus on membrane growth. *Nat. Cell Biol.* **5**, 103-108.

Lee, J. K., Brandin, E., Branton, D. and Goldstein, L. S. B. (1997). α-spectrin is required for ovarian follicle monolayer integrity in *Drosophila melanogaster*. *Development* **124**, 353-362.

Lietzke, S. E., Bose, S., Cronin, T., Klarlund, J., Chawla, A., Czech, M. P. and Lambright, D. G. (2000). Structural basis of 3-phosphoinositide recognition by pleckstrin homology domains. *Mol. Cell* **6**, 385-394.

Lombardo, C. R., Rimm, D. L., Kennedy, S. P., Forget, B. G. and Morrow, J. S. (1993). Ankyrin independent membrane sites for non-erythroid spectrin. *Mol. Biol. Cell* **4**, 57a.

Lopez-Schier, H. and St Johnston, D. (2002). Drosophila nicastrin is essential for the intramembranous cleavage of Notch. *Dev. Cell* **2**, 79-89.

Macoska, J. A., Xu, J., Ziemnicka, D., Schwab, T. S., Rubin, M. A. and Kotula, L. (2001). Loss of expression of human spectrin src homology domain binding protein 1 is associated with 10p loss in human prostatic adenocarcinoma. *Neoplasia* **3**, 99-104.

Marfatia, S. M., Morais-Cabral, J. H., Kim, A. C., Byron, O. and Chishti, A. H. (1997). The PDZ domain of human erythrocyte p55 mediates its binding to the cytoplasmic carboxyl terminus of glycophorin C. Analysis of

the binding interface by in vitro mutagenesis. *J. Biol. Chem.* **272**, 24191-24197.

McKeown, C., Pratis, V. and Austin, J. (1998). The *sma-1* gene encodes a β_{Heavy}-spectrin required for *C. elegans* morphogenesis. *Development* **125**, 2087-2098.

Medina, E., Williams, J., Klipfell, E., Zarnescu, D., Thomas, C. and le Bivic, A. (2002). Crumbs interacts with moesin and βHeavy-spectrin in the apical membrane skeleton of *Drosophila*. *J. Cell Biol.* **158**, 941-951.

Merilainen, J., Palovuori, R., Sormunen, R., Wasenius, V. M. and Lehto, V. P. (1993). Binding of the alpha-fodrin SH3 domain to the leading lamellae of locomoting chicken fibroblasts. *J. Cell Sci.* **105**, 647-654.

Michaely, P., Kamal, A., Anderson, R. G. and Bennett, V. (1999). A requirement for ankyrin binding to clathrin during coated pit budding. *J. Biol. Chem.* **274**, 35908-35913.

Moorthy, S., Chen, L. and Bennett, V. (2000). Caenorhabditis elegans beta-G spectrin is dispensable for establishment of epithelial polarity, but essential for muscular and neuronal function. *J. Cell Biol.* **149**, 915-930.

Munro, S. and Pelham, H. R. (1987). A C-terminal signal prevents secretion of luminal ER proteins. *Cell* **48**, 899-907.

Myat, M. M. and Andrew, D. J. (2002). Epithelial tube morphology is determined by the polarized growth and delivery of apical membrane. *Cell* **111**, 879-891.

Nelson, W. J., Shore, E. M., Wang, A. Z. and Hammerton, R. W. (1990). Identification of a membrane-cytoskeletal complex containing the cell adhesion molecule uvomorulin (E-cadherin), ankyrin, and fodrin in Mandin-Darby canine kidney epithelial cells. *J. Cell Biol.* **110**, 349-357.

Norman, K. R. and Moerman, D. G. (2002). Alpha spectrin is essential for morphogenesis and body wall muscle formation in Caenorhabditis elegans. *J. Cell Biol.* **157**, 665-677.

Pellikka, M., Tanentzapf, G., Pinto, M., Smith, C., McGlade, C. J., Ready, D. F. and Tepass, U. (2002). Crumbs, the Drosophila homologue of human CRB1/RP12, is essential for photoreceptor morphogenesis. *Nature* **416**, 143-149.

Pichaud, F. and Desplan, C. (2002). Cell biology: a new view of photoreceptors. *Nature* **416**, 139-140.

Polesello, C., Delon, I., Valenti, P., Ferrer, P. and Payre, F. (2002). Dmoesin controls actin-based cell shape and polarity during Drosophila melanogaster oogenesis. *Nat. Cell Biol.* **4**, 782-789.

Pradhan, D., Lombardo, C. R., Roe, S., Rimm, D. L. and Morrow, J. S. (2001). alpha-Catenin binds directly to spectrin and facilitates spectrin-membrane assembly in vivo. *J. Biol. Chem.* **276**, 4175-4181.

Rameh, L. E., Arvidsson, A., Carraway, K. L., III, Couvillon, A. D., Rathbun, G., Crompton, A., van Renterghem, B., Czech, M. P., Ravichandran, K. S., Burakoff, S. J. et al. (1997). A comparative analysis of the phosphoinositide binding specificity of pleckstrin homology domains. *J. Biol. Chem.* **272**, 22059-22066.

Rubin, G. M. and Spradling, A. C. (1982). Genetic transformation of Drosophila with transposable element vectors. *Science* **218**, 348-353.

Sako, Y. and Kusumi, A. (1995). Barriers for lateral diffusion of transferrin receptor in the plasma membrane as characterized by receptor dragging by laser tweezers: fence versus tether. *J. Cell Biol.* **129**, 1559-1574.

Speck, O., Hughes, S. C., Noren, N. K., Kulikauskas, R. M. and Fehon, R. G. (2003). Moesin functions antagonistically to the Rho pathway to maintain epithelial integrity. *Nature* **421**, 83-87.

Speicher, D. W. and Marchesi, V. T. (1984). Erythrocyte spectrin is comprised of many homologous triple helical segments. *Nature* **311**, 177-180.

Tepass, U. and Hartenstein, V. (1994). The development of cellular junctions in the *Drosophila* embryo. *Dev. Biol.* **161**, 563-596.

Tepass, U., Gruszynski-DeFeo, E., Haag, T. A., Omatyar, L., Török, T. and Hartenstein, V. (1996). *shotgun* encodes *Drosophila* E-cadherin and is preferentially required during cell rearrangement in the neurectoderm and other morphogenetically active epithelia. *Genes Dev.* **10**, 672-685.

Thomas, C. M. and Kiehart, D. P. (1994). Beta heavy-spectrin has a restricted tissue and subcellular distribution during Drosophila embryogenesis. *Development* **120**, 2039-2050.

Thomas, C. M. and Williams, J. A. (1999). Dynamic rearrangement of the spectrin membrane skeleton during the generation of epithelial polarity in Drosophila. *J. Cell Sci.* **112**, 2843-2852.

Thomas, C. M., Zarnescu, D. C., Juedes, A. E., Bales, M. A., Londergan, A., Korte, C. C. and Kiehart, D. P. (1998). Drosophila β_{Heavy}-spectrin is essential for development and contributes to specific cell fates in the eye. *Development* **125**, 2125-2134.

Thomas, G. H. (2001). Spectrin: The ghost in the machine. *BioEssays* **23**, 152-160.

Thomas, G. H., Newbern, E. C., Korte, C. C., Bales, M. A., Muse, S. V., Clark, A. G. and Kiehart, D. P. (1997). Intragenic duplication and divergence in the spectrin superfamily of proteins. *Mol. Biol. Evol.* **14**, 1285-1295.

Touhara, K., Koch, W. J., Hawes, B. E. and Lefkowitz, R. J. (1995). Mutational analysis of the pleckstrin homology domain of the beta-adrenergic receptor kinase. Differential effects on G beta gamma and phosphatidylinositol 4,5-bisphosphate binding. *J. Biol. Chem.* **270**, 17000-17005.

Tse, W. T., Lecomte, M.-C., Costa, F. F., Garbarz, M., Feo, C., Boivin, P., Dhermy, D. and Forget, B. G. (1990). Point mutation in the β-spectrin gene associated with αI/74 hereditary elliptocytosis. *J. Clin. Invest.* **86**, 909-916.

Tse, W. T., Tang, J., Jin, O., Korsgren, C., John, K. M., Kung, A. L., Gwynn, B., Peters, L. L. and Lux, S. E. (2001). A new spectrin, beta IV, has a major truncated isoform that associates with promyelocytic leukemia protein nuclear bodies and the nuclear matrix. *J. Biol. Chem.* **276**, 23974-23985.

Uemura, T., Oda, H., Kraut, R., Hayashi, S., Kataoka, Y. and Takeichi, M. (1996). Zygotic DE-cadherin expression is required for processes of dynamic epithelial cell rearrangement in the *Drosophila* embryo. *Genes Dev.* **10**, 659-671.

Wharton, K. A., Yedvobnick, B., Finnerty, V. G. and Artavanis-Tsakonas, S. (1985). opa: a novel family of transcribed repeats shared by the *Notch* locus and other developmentally regulated loci in *D. melanogaster*. *Cell* **40**, 55-62.

Yeaman, C., Grindstaff, K. and Nelson, W. J. (1999). New perspectives on mechanisms involved in generating epithelial cell polarity. *Physiol. Rev.* **79**, 73-98.

Zarnescu, D. C. (2000). On the role of β_H spectrin during epithelial development in *Drosophila melanogaster*, PhD thesis. In *Department of Biochemistry and Molecular Biology*, pp. 227. University Park: The Pennsylvania State University.

Zarnescu, D. C. and Thomas, C. M. (1999). Apical spectrin is essential for epithelial morphogenesis but not apicobasal polarity in Drosophila. *J. Cell Biol.* **146**, 1075-1086.

Zhang, P., Talluri, S., Deng, H., Branton, D. and Wagner, G. (1995). Solution structure of the pleckstrin homology domain of Drosophila beta-spectrin. *Structure* **3**, 1185-1195.